2026 IEEE International Conference on Robotics and Automation (ICRA 2026)
June 1-5, 2026. Vienna, Austria

# Mechanomyography-Based Closed-Loop Control of FES Enabling Prolonged Force Assistance by Monitoring Muscle Fatigue

Zehao Liu[1], Weiguang Huo[2,3] and Ravi Vaidyanathan[1]

***Abstract*— Functional Electrical Stimulation (FES) is a critical therapy for motor rehabilitation, yet the rapid onset of muscle fatigue severely limits its efficacy. This paper presents the design, implementation, and validation of a comprehensive, intelligent closed-loop FES system designed to provide effective force assistance by actively sensing FES-induced fatigue. The system integrates a pressure-based Mechanomyography (P_MMG) sensor for real-time feedback of muscle force capacity, a Kalman filter for robust signal estimation, and a fuzzy-logic-based Proportional-Integral-Derivative (PID) controller to modulate FES dynamically. The developed system was first validated in a comprehensive simulation and then tested with four healthy participants. The results demonstrate that the closed-loop fuzzy PID controller yielded a functionally meaningful improvement in performance over an open-loop-controlled protocol. The system substantially extended the duration of effective FES and, critically, delayed the onset of functional failure (indicated by a force drop $> 50\%$), with performance improvements showing a strong trend toward statistical significance (Wilcoxon signed-rank test, $p = 0.0625$). This work delivers a practical and effective solution for managing fatigue during FES therapy, holding the potential to significantly enhance rehabilitation outcomes.**

***Keywords*—Functional Electrical Stimulation (FES), Neuromuscular Fatigue, Mechanomyography (MMG), Closed-Loop Control, Fuzzy PID, Kalman Filter.***

## I. INTRODUCTION

Functional Electrical Stimulation (FES) is a cornerstone of neurorehabilitation, using low-frequency electrical pulses to restore motor function in individuals with neurological impairments such as stroke or spinal cord injury [1], [2]. Its clinical importance is underscored by the growing global health burden of conditions like stroke, which affected nearly 90 million people in 2020, with two-thirds of survivors suffering from walking impairments [3]. However, the therapeutic potential of FES is often curtailed by a significant limitation: FES-induced muscle contractions cause muscles to fatigue very rapidly, far more so than during voluntary contractions [4], [5]. This premature fatigue diminishes the effectiveness of rehabilitation, limits the duration of functional tasks, and reduces the overall therapeutic dose that can be delivered in a session [6], [7].

A key obstacle in managing this fatigue is the lack of a reliable, non-invasive monitoring tool. Electromyography (EMG), the gold standard for measuring muscle activity, is rendered unusable during FES because the electrical stimulation pulses overwhelm the physiological signal [8], [9]. To address this, Mechanomyography (MMG), which records the mechanical vibrations of contracting muscle fibers, has emerged as a promising, artifact-immune alternative [10], [11]. MMG captures the mechanical output of muscle activity, providing a direct window into the muscle's functional state even during active stimulation [12]. Despite MMG's potential, translating it into a functional closed-loop system still faces several knowledge gaps. First, there is a lack of quantitative characterization of FES fatigue during dynamic, functionally relevant movements [13]. Second, a significant gap exists for practical, real-time fatigue prediction models driven by wearable biosensors rather than impractical laboratory measurements [14]. Finally, intelligent closed-loop control systems that can actively manage fatigue to maintain therapeutic efficacy, rather than simply shutting down, are critically needed but remain rare [15], [16].

To address these challenges, this paper presents the design, implementation, and in-vivo validation of a complete, intelligent closed-loop FES system that actively manages fatigue. Our system integrates three key components. First, it utilizes a pressure-based Mechanomyography (P_MMG) sensor for direct physiological feedback. This sensor is part of a novel dual-modality system developed in foundational work, where a quantitative analysis demonstrated the P_MMG signal's superiority for fatigue tracking due to its strong, monotonic correlation with force decline [17]. Second, it employs a Kalman filter for robust real-time signal estimation. Finally, a Fuzzy Proportional-Integral-Derivative (PID) controller dynamically modulates FES parameters. This work represents a full engineering solution to the challenge of FES-induced fatigue, demonstrating a substantial extension of therapeutic duration in human trials.

The remainder of this paper is organized as follows: Section II details the system architecture, including the P_MMG sensing, Kalman filtering, and Fuzzy PID control design. Section III describes the human experimental protocol. Section IV presents the experimental results and statistical analysis. Section V discusses the implications of the findings, and Section VI concludes the paper.

This work was supported in part by the UK EPSRC (EP/R511547/1), the UK Dementia Research Institute (DRI) (DRI-XCPP2022-013), and the UK NIHR (NIHR202133). This work was also supported by the UK Dementia Research Institute (award numbers UK DRI-7003 and UK DRI-7005) through UK DRI Ltd, principally funded by the Medical Research Council, and additional funding partner Alzheimer's Society, as well as the National Natural Science Foundation of China (Grant 62373202) and the Fundamental Research Funds for the Central Universities of China.

[1]Department of Mechanical Engineering, Imperial College London, London, United Kingdom (b.liu21@imperial.ac.uk; r.vaidyanathan@imperial.ac.uk).

[2]College of Artificial Intelligence, Nankai University, Tianjin, China (weiguang.huo@nankai.edu.cn).

[3]Institute of Intelligent Technology and Robotic Systems, Shenzhen Research Institute, Nankai University, Shenzhen, China.

## II. METHODS

The closed-loop control system is designed to actively manage FES-induced muscle fatigue through real-time feedback. Its architecture, depicted in Fig. 1, comprises three main stages: a sensing and estimation pipeline, an intelligent control block, and a safety protocol.

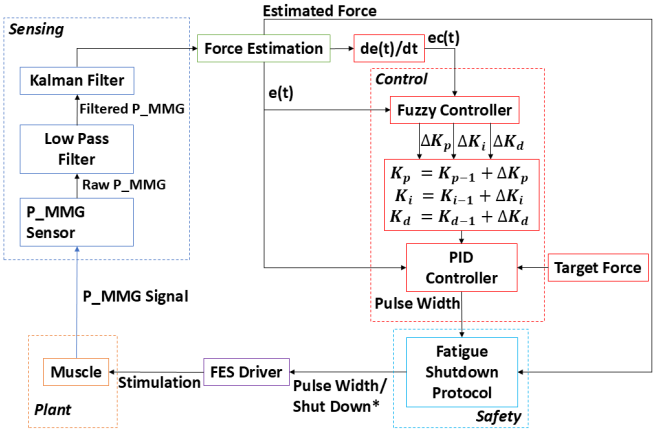


Fig. 1: Diagram of the proposed closed-loop control system, illustrating the Sensing (Kalman Filter), Control (Fuzzy PID), and Safety (Shutdown Protocol) stages.

### A. Feedback Sensor and Signal Selection

The feedback for the control system is derived from a novel, dual-modality Mechanomyography (MMG) sensor, shown in Fig. 2. This sensor was designed to robustly monitor muscle activity during FES by capturing different mechanical aspects of muscle contraction.

The sensor integrates two distinct components within a single compact housing: a piezoresistive pressure sensor (P_MMG) and a microphone (M_MMG). The P_MMG component is designed to be sensitive to low-frequency, bulk deformation of the muscle belly, which occurs during contraction. It measures these gross shape changes through a soft silicone interface. In contrast, the M_MMG component is an acoustic sensor with a reported Signal-to-Noise Ratio (SNR) of 45 dB that captures higher-frequency surface vibrations generated by the oscillation of muscle fibers. The P_MMG sensor's response was validated using a materials testing system (INSTRON 5900), which demonstrated a near-linear relationship between the sensor's output and applied force, with a maximum coefficient of variation of only 0.21% across repeated tests and a high SNR of 88 dB [17].

A critical finding from prior research was the difference in signal reliability for tracking FES-induced fatigue. A quantitative analysis showed that the P_MMG signal consistently and monotonically decreased with fatigue, exhibiting a strong, linear correlation with the decline in muscle force ($\bar{r} = 0.740$ in control subjects). Conversely, the M_MMG signal often displayed non-monotonic behavior (e.g., decreasing then increasing), resulting in weaker and inconsistent correlations with force decline. The significantly higher SNR of the P_MMG sensor further explains its superior stability and makes it a more reliable input for a feedback controller [17]. Therefore, for the following development of this closed-loop system, the robust and reliable P_MMG signal was selected as the sole feedback source.

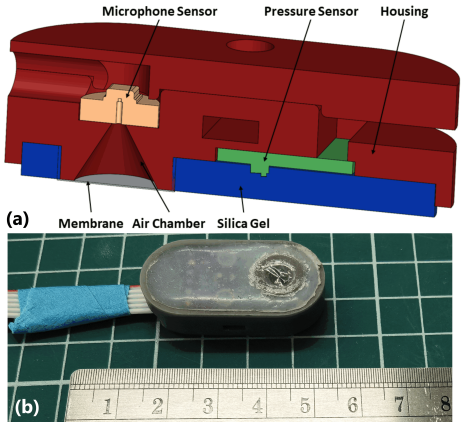


Fig. 2: The dual-modality MMG sensor used in this study. (a) Schematic showing the microphone and pressure sensor components. (b) Photograph of the fabricated sensor [17].

### B. Closed-Loop Control Architecture

The control architecture is composed of three main stages: a sensing and state estimation pipeline, an intelligent control block, and an integrated safety protocol. Each stage is designed to work in sequence to provide robust, adaptive, and safe FES.

*1) Sensing and State Estimation Pipeline:* The sensing pipeline begins by processing the raw P_MMG signal. For each processing window, the signal is first passed through a low-pass filter, and its mean value is calculated. To correct for the sensor's inherent non-zero reading at rest, a pre-configured static pressure offset is then subtracted. This calibrated value is subsequently fed into a Kalman filter for optimal state estimation. The filter operates through a predict-update cycle.

**Prediction Step:** The filter predicts the current state ($\hat{x}_{k|k-1}$) based on the previous state estimate:

$$\hat{x}_{k|k-1} = A\hat{x}_{k-1|k-1} + Bu_{k-1} \quad (1)$$

$$P_{k|k-1} = AP_{k-1|k-1}A^T + Q \quad (2)$$

**Update Step:** The filter corrects the prediction using the current measurement ($z_k$):

$$K_k = P_{k|k-1}H^T(HP_{k|k-1}H^T + R)^{-1} \quad (3)$$

$$\hat{x}_{k|k} = \hat{x}_{k|k-1} + K_k(z_k - H\hat{x}_{k|k-1}) \quad (4)$$

$$P_{k|k} = (I - K_kH)P_{k|k-1} \quad (5)$$

For filtering the scalar P_MMG signal, this model is simplified: the state transition matrix $A = 1$, the observation matrix $H = 1$, and there is no control input ($Bu_{k-1} = 0$). The process noise covariance $Q$ and measurement noise covariance $R$ are the key tuning parameters. This filtering process yields a smooth and reliable signal, hereafter termed

TABLE I: Fuzzy Inference Rule Bases for PID Gain Adjustments ($\Delta K_p, \Delta K_i, \Delta K_d$)

| $e(t)$ | $ec(t)$ | | | | |
|---|---|---|---|---|---|
| | **NB** | **NS** | **ZE** | **PS** | **PB** |
| $\Delta K_p$ **Rule Base** | | | | | |
| **NB** | PB | PB | PS | PS | ZE |
| **NS** | PB | PS | PS | ZE | NS |
| **ZE** | PS | PS | ZE | NS | NS |
| **PS** | ZE | NS | NB | NB | NB |
| **PB** | NS | NB | NB | NB | NB |
| $\Delta K_i$ **Rule Base** | | | | | |
| **NB** | NB | NB | NS | NS | ZE |
| **NS** | NB | NS | NS | ZE | PS |
| **ZE** | NS | ZE | PS | PS | ZE |
| **PS** | ZE | PS | ZE | NS | NS |
| **PB** | PS | ZE | ZE | NS | NB |
| $\Delta K_d$ **Rule Base** | | | | | |
| **NB** | ZE | PS | PB | PB | PS |
| **NS** | NS | ZE | PS | PS | ZE |
| **ZE** | NB | NS | ZE | ZE | NS |
| **PS** | NB | NB | NS | NS | NS |
| **PB** | NB | NB | NB | NB | NB |

NB: Negative Big, NS: Negative Small, ZE: Zero, PS: Positive Small, PB: Positive Big.

the 'Estimated Force'. To map this physical pressure signal to a dimensionless fatigue index required for the controller, we employ a dynamic normalization strategy. The initial stable P_MMG reading recorded during the first stimulated contraction (fresh muscle state) is captured as the baseline capacity ($P_{ref}$). The real-time fatigue level $F(t)$ is then defined as the ratio of the current filtered signal to this baseline: $F(t) = \frac{\hat{x}_{k|k}}{P_{ref}} \times 100\%$. This normalized metric serves as the process variable for the PID loop. This mapping strategy is grounded in our recent validation study, which demonstrated that the P_MMG signal exhibits a strong linear correlation with isometric muscle force decline in both healthy ($\bar{r} = 0.740$) and post-stroke ($\bar{r} = 0.928$) populations [17], confirming its validity as a robust surrogate for real-time fatigue monitoring.

*2) Fuzzy PID Controller:* To counteract the decline in the muscle's output due to fatigue, this study employs a Fuzzy PID controller to dynamically adjust the FES Pulse Width. A conventional PID controller with fixed gains is often insufficient for FES applications due to the significant non-linearities and time-varying characteristics of muscle fatigue. The Fuzzy PID controller addresses this challenge by combining the reasoning capabilities of fuzzy logic with the robustness of a traditional PID controller. The core principle is to use fuzzy "IF-THEN" rules to online-tune the PID gains ($K_p, K_i, K_d$), enabling an adaptive response to the muscle's changing state.

The controller's primary goal is to maintain the normalized 'Estimated Force' at a desired target level. The inputs to the fuzzy inference system are the error $e(t)$ and its rate of change, $ec(t)$. The system's outputs are the calculated adjustments ($\Delta K_p, \Delta K_i, \Delta K_d$) for the PID gains. The control process involves these steps:

1) **Fuzzification:** Crisp inputs $e(t)$ and $ec(t)$ are converted into fuzzy sets (e.g., Negative Big (NB), Zero (ZE), Positive Big (PB)) using triangular membership functions.
2) **Fuzzy Inference:** A 5x5 "IF-THEN" rule base determines the required adjustments for each gain. The system employs the Mamdani-type inference method, where the firing strength of each rule is calculated using the 'min' operator for the fuzzy 'AND' logic.
3) **Defuzzification:** The aggregated fuzzy output is converted into a crisp numerical value using the Centroid of Area (CoA) method, yielding the final adjustment values: $\Delta K_p, \Delta K_i, \Delta K_d$.
4) **PID Parameter Update:** The gains for the current control cycle ($K_p'$, $K_i'$, $K_d'$) are updated by adding the fuzzy adjustments to a set of base parameters.
5) **Pulse Width Calculation:** To address the potential contradiction noted by reviewers regarding the PID form, we explicitly implement an incremental (velocity-form) PID algorithm. The controller calculates the increment in pulse width, $\delta u(t)$, using the positional PID law with updated gains based on the error $e(t)$:

$$\delta u(t) = K_p' e(t) + K_i' \int e(t)dt + K_d' \frac{de(t)}{dt} \quad (6)$$

This output is then applied as an incremental update to the FES pulse width from the previous time step:

$$PW(t) = PW(t-1) + \delta u(t) \quad (7)$$

This formulation combines the intuitive tuning of positional PID with the smooth, integral-action behavior of an incremental implementation, ensuring stable transitions when gains are adapted.

This adaptive mechanism allows for a robust response to the non-linear and time-varying characteristics of muscle fatigue.

*3) Safety Protocol:* A critical safety protocol is integrated to prevent prolonged and ineffective stimulation of a non-responsive muscle. The system halts stimulation only when two conditions are met simultaneously: the FES pulse width is being commanded at its maximum value, and the normalized 'Estimated Force' is concurrently below a critical shutdown threshold for a predefined number of consecutive cycles (n).

### *C. Hardware and Implementation*

The system was implemented on a custom-designed, programmable FES platform, centered around an STM32 microcontroller and programmed in C++ using the Mbed OS. The P_MMG sensor was interfaced via I2C, sampling at 157 Hz to ensure high temporal resolution for the feedback loop.

A key feature is the dynamic parameter configuration via a single structured JSON file on an SD card. This allows for on-site tuning of all system parameters—including Kalman filter covariances ($Q, R$), Fuzzy PID rules, FES limits (pulse width, amplitude), and safety thresholds—without needing to recompile the firmware. This strategy dramatically improves experimental flexibility and facilitates a more streamlined transition from laboratory research to real-world use.

### D. System Validation via Simulation

Before human trials, a computer simulation was developed in Python to validate the proposed closed-loop control architecture in a safe and repeatable environment. The objectives were to verify the logical state transitions and assess the dynamic performance of the Fuzzy PID controller. The simulation was configured using the core system parameters detailed in Table II.

A challenging synthetic P_MMG signal was generated to test the controller's capabilities, emulating a rapid initial decline, a prolonged period of high-amplitude oscillations around the target threshold, and a final decay representing complete muscle exhaustion. The simulation results successfully validated the entire control strategy. The simulation results, shown in Fig. 3, successfully validated the entire control strategy. The top panel illustrates the system's response to a synthetic P_MMG signal (blue line). The Kalman filter generated a smooth estimate (red line), which the controller used to track the 70% target value. The background color indicates the system's correct transitions between Monitoring, PID Control, and Shutdown states. The bottom panel displays the corresponding FES pulse width, showing how the controller actively modulated the stimulation to counteract signal fluctuations and maintain the target.

The internal workings of the Fuzzy PID controller are detailed in Fig. 3(c). The top three panels show the real-time adjustments to the proportional ($K_p$), integral ($K_i$), and derivative ($K_d$) gains. The solid lines track the absolute value of each gain, while the vertical bars indicate whether the fuzzy logic system commanded an increase (green) or a decrease (red) in response to error. The bottom panel shows the resulting FES pulse width output. This demonstrates the controller's dynamic and adaptive nature.

TABLE II: Configuration Parameters of the Closed-Loop Control FES System

| Category | Parameter | Value |
|---|---|---|
| Kalman Filter | Process Noise Covariance (Q) | 10.0 |
| | Measurement Noise Covariance (R) | 10.0 |
| Fuzzy PID Controller | Base Gain ($K_p, K_i, K_d$) | 14.0, 4.0, 0.5 |
| | Delta Scale ($\Delta K_p, \Delta K_i, \Delta K_d$) | 5.0, 1.0, 0.2 |
| | Error Universe ($e$) | [-0.5, 0.5] |
| | Error Change Universe ($ec$) | [-0.15, 0.15] |
| Control & Safety Protocol | Pulse Width Range | 90 – 360 $\mu$s |
| | Target Value | 70% of initial P_MMG |
| | Shutdown Threshold | 50% of initial P_MMG |
| | Shutdown Cycles (n) | 4 |

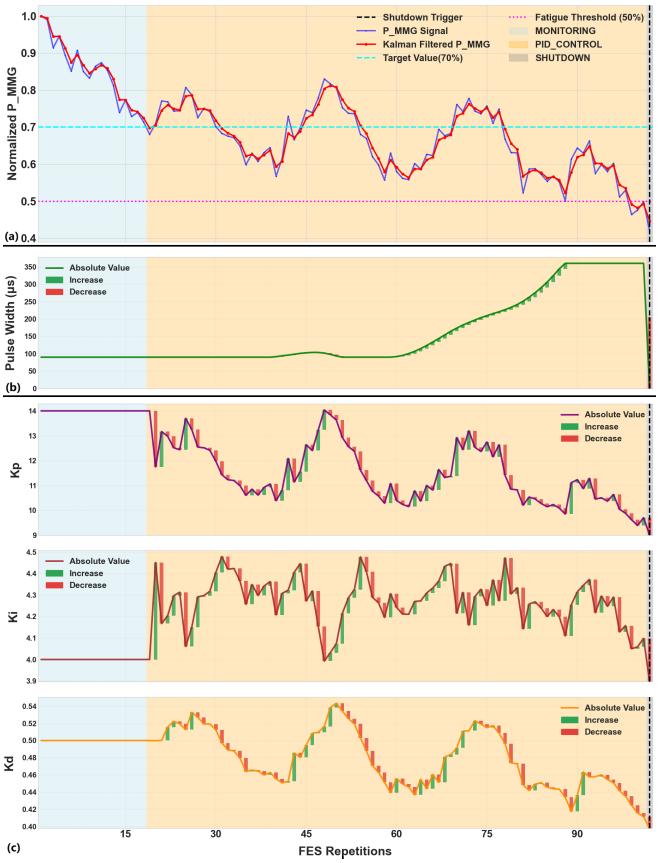


Fig. 3: Simulation results. (a) Kalman estimate (red) tracking the target signal. (b) FES Pulse Width output. (c) Real-time adaptive tuning of PID gains ($K_p, K_i, K_d$).

## III. Human Experimental Protocol

### A. Participants

Four healthy volunteers (three males and one female, mean age: $27.75 \pm 2.06$ years) were recruited from a local university population. Participants did not present any gait abnormalities or perform physical exercise within 24 hours of the experiment. All experiments were approved by the Imperial College Research Committee (ICREC: 15IC3068), and all participants provided signed informed consent.

### B. Setup and Protocol

As shown in Fig. 4, participants were seated on an adapted chair with their dominant leg placed and fixed on a custom-made ergometer, which was equipped with a pulley system and a load cell (HYchuangan LTD) to ensure accurate isometric force measurements. The ankle joint was maintained at approximately 110°, a neutral position [18], with the foot fixed to a support connected to a load cell to measure isometric dorsiflexion force.

The Tibialis Anterior (TA) muscle belly was located via palpation during a voluntary contraction. The MMG sensor was then affixed over this area using an elastic strap, with the strap's tightness adjusted to ensure the P_MMG sensor reading stabilized between 108 kPa and 110 kPa for consistent contact pressure. Two FES surface electrodes were

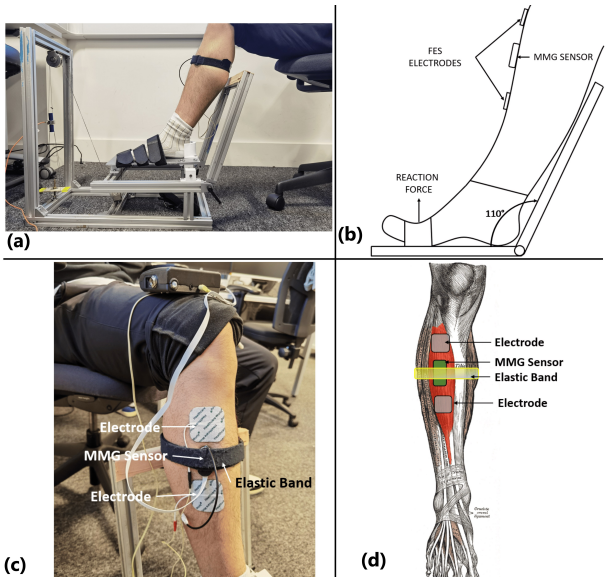


Fig. 4: Lower limb experimental setup. (a) Overall view. (b) Muscle and hardware schematic. (c) Sensor/electrode placement. (d) Hardware schematic. Key: Red (electrodes), Green (MMG), Yellow (band).

placed at the proximal and distal regions of the TA muscle belly, avoiding tendinous tissue.

The fatigue protocol consisted of intermittent FES for up to 10 minutes (4s stimulation, 1s rest). FES frequency and voltage were constant (25 Hz, 35 V). The closed-loop system dynamically adjusted the pulse width to maintain the P_MMG-derived 'Estimated Force' at its target level. The key control and safety parameters, such as the pulse width range (90-360 $\mu$s), target value (70%), and shutdown criteria, are specified in Table II. The experiment would conclude either upon reaching the 10-minute mark or when the fatigue shutdown protocol was triggered. This safety condition was met if the 'Estimated Force' remained below 50% of its initial peak for 4 consecutive cycles while the controller was commanding the maximum pulse width (360 $\mu$s), ensuring that prolonged, ineffective stimulation was not applied to a non-responsive muscle. For performance comparison, a non-PID (open-loop) protocol was also conducted for each participant. In this condition, all stimulation parameters (frequency at 25 Hz, voltage at 35 V) were identical to the closed-loop trial; however, the pulse width was held constant at its initial value of 90 µs throughout the entire session, with no feedback-based adjustments. This protocol serves as a baseline to represent a standard, non-adaptive FES application.

## IV. RESULTS

To systematically evaluate the performance of the closed-loop Fuzzy PID control system, a quantitative comparison was made against a non-PID (no feedback) protocol. The results are presented beginning with a summary of key performance metrics, followed by a detailed graphical analysis of representative participants.

### A. Quantitative Performance Summary

The closed-loop Fuzzy PID controller demonstrated a notable improvement over the non-PID protocol, as summarized in Table III. Due to the small sample size (N=4), the non-parametric Wilcoxon signed-rank test was used for all statistical comparisons to ensure robustness.

The PID control showed a strong trend towards extending the total number of FES repetitions. The median number of repetitions increased from 36.5 (non-PID) to 77.5 (PID), representing a 112% increase at the median. While falling just short of the conventional threshold for statistical significance, the data reveals a clear and functionally meaningful improvement (Wilcoxon signed-rank test, p = 0.0625).

More critically, the controller showed a strong trend in delaying the onset of functional failure (a force drop $>$ 50%). For the non-PID protocol, the median number of repetitions before failure was 25. In contrast, under PID control, two participants fatigued rapidly (at 30 and 35 repetitions, respectively), while the other two high-endurance participants completed the entire 120-repetition session without reaching the failure threshold. This demonstrates a substantial extension of functional performance, with the improvement approaching statistical significance (Wilcoxon signed-rank test, p = 0.0625). The cumulative normalized force, representing the total work performed, also showed a strong positive trend, increasing by an average of 82.4%.

### B. Graphical Analysis of Individual Performance

The system's adaptive performance was evident across all participants. We present the graphical analysis for three representative cases (P1, P2, and P4) to illustrate the controller's robustness across diverse physiological profiles: rapid fatigue, dynamic recovery, and high endurance.

*1) Rapid Fatigue Profile (Participant 1 & 3):* Participant 1 serves as the primary example of a rapid fatigue profile, likely associated with a higher proportion of fast-twitch muscle fibers. As shown in Fig. 5(a), the controller actively counteracted the declining muscle output by steadily increasing the FES pulse width from 90 $\mu$s to its maximum of 360 $\mu$s.

The comparison in Fig. 5(b) highlights the benefit of this strategy: the PID-controlled trial sustained functional force for 35 repetitions, while the non-PID trial's force dropped below the 50% threshold after only 15 repetitions, thus more than doubling the effective therapeutic duration.

TABLE III: Summary of Performance: PID vs. non-PID

| Participant | Metric | PID | non-PID | Change |
|---|---|---|---|---|
| P1 | Total Reps | 35 | 23 | +12 |
| | Reps at 50% Drop | 35 | 15 | +20 |
| P2 | Total Reps | 120 | 48 | +72 |
| | Reps at 50% Drop | >120* | 34 | >+86 |
| P3 | Total Reps | 35 | 25 | +10 |
| | Reps at 50% Drop | 30 | 16 | +14 |
| P4 | Total Reps | 120 | 94 | +26 |
| | Reps at 50% Drop | >120* | 76 | >+44 |

*Force did not drop below 50% before session concluded.

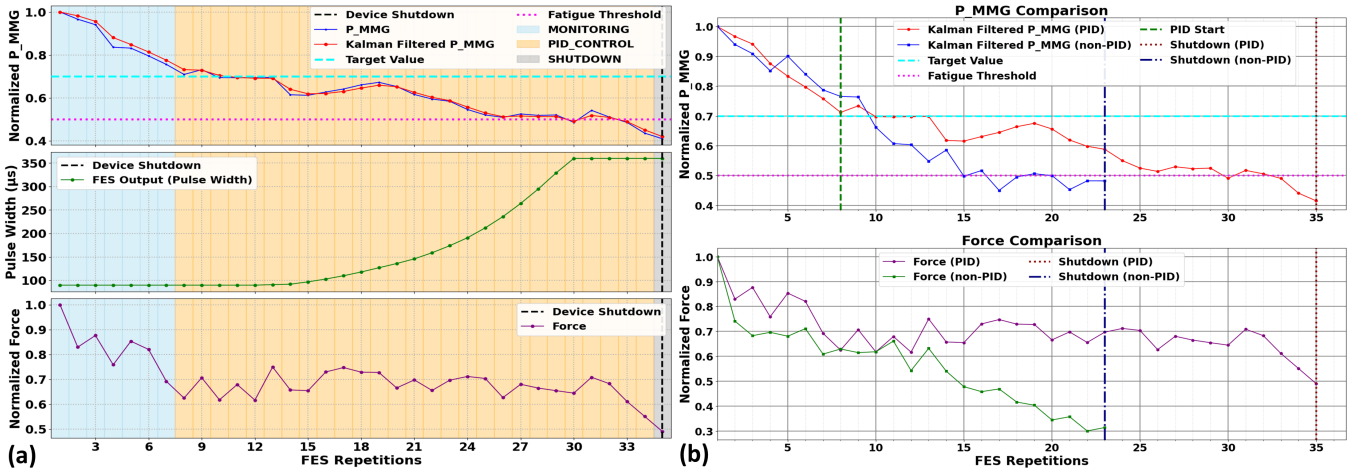


Fig. 5: Participant 1 (Rapid Fatigue). (a) Controller increases pulse width to maintain target. (b) PID significantly delays functional failure vs. non-PID.

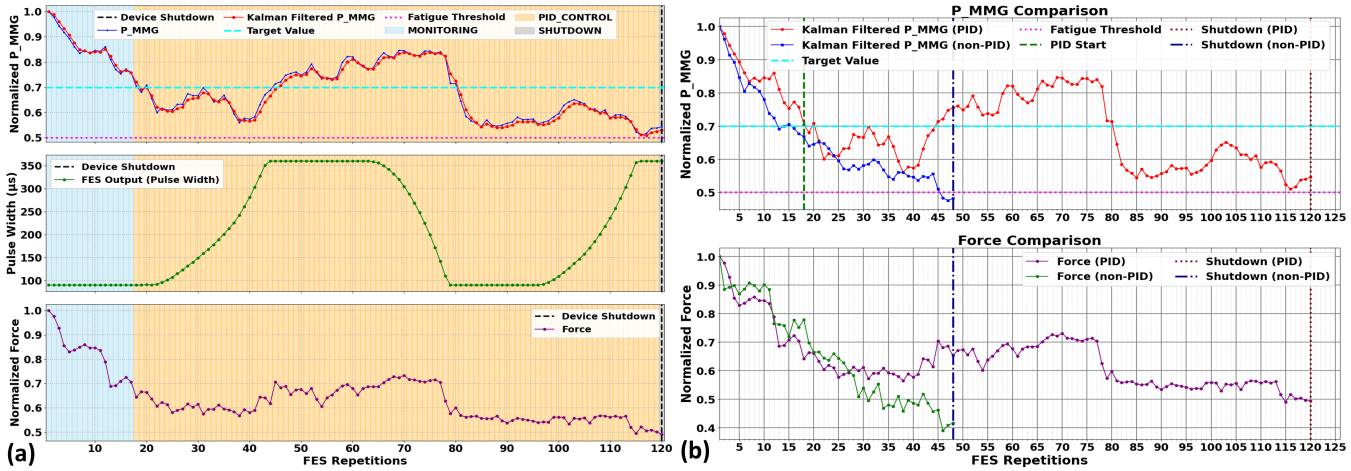


Fig. 6: Participant 2 (Dynamic Recovery). (a) Controller adapts to mid-session recovery. (b) PID extends therapeutic duration vs. early non-PID failure.

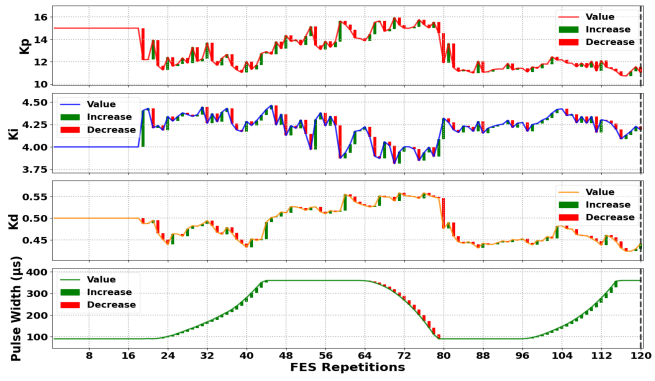


Fig. 7: Dynamic gain tuning for Participant 2, illustrating the controller's response to physiological recovery.

Participant 3 exhibited a very similar rapid fatigue trend. Although graphical details are omitted for brevity, the numerical performance confirmed the same pattern (Table III). The PID controller delayed functional failure from 16 repetitions (non-PID) to 30 repetitions (PID), reinforcing the consistency of the strategy for fatigue-prone individuals.

*2) Dynamic Recovery Profile (Participant 2):* The data from Participant 2 showcases the system's ability to handle complex physiological dynamics. The controller successfully managed the entire 120-repetition session (Fig. 6(a)). Notably, this participant exhibited a mid-session recovery phase. The controller demonstrated advanced adaptability by first increasing, then decreasing, and finally increasing the pulse width again to match the muscle's fluctuating state. The comparison in Fig. 6(b) is stark: the PID-controlled session completed the full duration without functional failure, whereas the non-PID trial failed after only 48 repetitions.

The advanced adaptability for Participant 2 is further detailed in Fig. 7. Similar to the simulation results, the Fuzzy PID system dynamically tuned the gains in real-time. For instance, during the recovery phase (approx. reps 75-85), as the muscle's output naturally increased, the fuzzy logic system commanded a significant decrease in the gains to avoid over-stimulation.

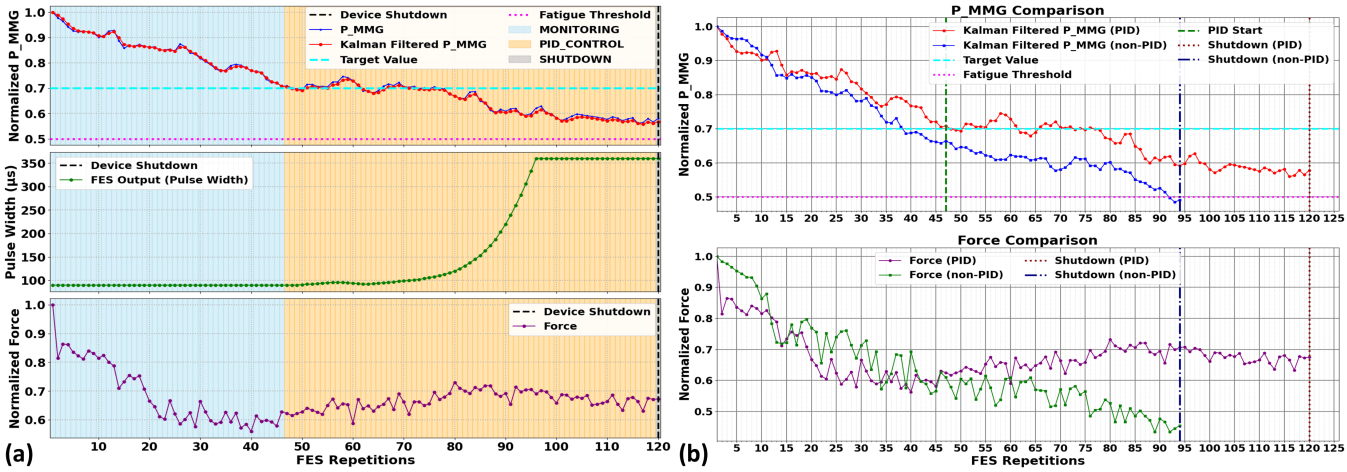


Fig. 8: Participant 4 (High Endurance). (a) Sustained performance for full 10-min session. (b) PID prevented functional failure vs. non-PID trial.

*3) High Endurance Profile (Participant 4):* The results for Participant 4 reinforce the system's effectiveness for users with high endurance, likely indicative of Type I fiber dominance. The PID controller successfully maintained the muscle's force output above the 50% functional failure threshold for the entire 120-repetition session by modulating the pulse width as needed (Fig. 8(a)). In contrast, the comparison in Fig. 8(b) shows the non-PID trial failing at 94 repetitions, demonstrating that even for less fatigable individuals, the intelligent feedback loop is critical for preventing eventual failure and maximizing session duration.

## V. DISCUSSION

The central finding of this study is that the intelligent, P_MMG-based closed-loop control system provides a functionally meaningful improvement in managing FES-induced fatigue, with results showing a strong trend toward statistical significance ($p$ = 0.0625). The system's ability to substantially delay the onset of functional failure (force drop $>$ 50%) directly addresses one of the most significant barriers to FES efficacy [6]. By prolonging this therapeutic window, the system creates a greater opportunity for the high-repetition, task-specific practice that is essential for driving neuroplasticity and long-term motor recovery [19].

The system's success is distinguished by its unique combination of a direct physiological marker of peripheral fatigue (P_MMG) with an intelligent, adaptive controller. Unlike systems that rely on indirect kinematic feedback for tasks like gait control [20], or those that require complex artifact cancellation for EMG feedback [21], the use of the validated P_MMG signal provides a direct, non-invasive, and artifact-immune window into the muscle's force-generating capacity. The system's robustness is further enhanced by the Kalman filter, which proved critical in providing a smooth, reliable estimate from the noisy raw P_MMG signal. Without this filtering, the derivative term of a PID controller would amplify noise, leading to unstable output.

Building on this, the Fuzzy PID controller demonstrated its exceptional capability in handling the non-linear dynamics of the neuromuscular system. A key observation from the human trials was the significant variability in fatigue rates among participants. This likely reflects fundamental differences in individual physiology, particularly the composition of muscle fiber types [22], [23]; individuals with a higher proportion of fast-twitch (Type II) fibers fatigue more rapidly under FES than those with more fatigue-resistant slow-twitch (Type I) fibers. This inherent variability underscores the inadequacy of a "one-size-fits-all" FES approach [24]. The Fuzzy PID system provides an elegant solution by functioning as an implicit personalization engine. As shown in the dynamic gain tuning figures (e.g., Fig. 7), the controller appropriately adjusted its parameters in real-time in response to both gradual fatigue and rapid physiological fluctuations, effectively delivering a personalized intervention without requiring prior physiological modeling.

In a clinical context, such as foot drop correction post-stroke, delaying the 50% force drop threshold is critical. This threshold represents the functional point below which the Tibialis Anterior can no longer provide adequate foot clearance during the swing phase of gait, increasing the risk of tripping [25]. Crucially, foundational work has already demonstrated that the P_MMG signal exhibits a comparable monotonic decline with fatigue in stroke survivors as it does in healthy individuals [17]. Therefore, we are optimistic that this closed-loop control system holds significant potential for effective application in stroke rehabilitation to enable longer and potentially more effective gait training sessions.

While this work demonstrates a functional proof-of-concept, its limitations define a clear roadmap for future research. First, the validation was conducted during isometric contractions; a critical next step is to validate the system's performance during dynamic activities such as FES-assisted cycling or walking [26]. Second, the system was tested on a small cohort of healthy volunteers. To confirm its clinical utility, larger-scale trials in target patient populations, such as stroke survivors, are imperative, as their neuromuscular

response can be significantly different [27], [28]. Finally, future work could explore machine learning or reinforcement learning algorithms to develop even more customized and predictive control policies [29].

## VI. CONCLUSION

This paper successfully demonstrated the design, implementation, and in-vivo validation of an intelligent closed-loop FES system. By integrating a novel P_MMG sensor, a Kalman filter, and a Fuzzy PID controller, the system demonstrated clear superiority over non-controlled FES in managing muscle fatigue. The key outcomes were a substantial extension of effective muscle stimulation and a robust delay in the onset of functional failure. This work delivers a complete and practical engineering solution to the critical challenge of FES-induced fatigue and holds tangible potential to enhance the efficacy of motor rehabilitation for individuals with neurological impairments.

## REFERENCES


[1] C. Marquez-Chin and M. R. Popovic, "Functional electrical stimulation therapy for restoration of motor function after spinal cord injury and stroke: a review," *BioMedical Engineering OnLine*, vol. 19, no. 1, p. 34, May 2020.

[2] D. Bhatia, G. Bansal, R. Tewari, and K. Shukla, "State of art: Functional electrical stimulation (fes)," *International Journal of Biomedical Engineering and Technology*, vol. 5, no. 1, pp. 77–99, 2011.

[3] C. W. Tsao, A. W. Aday, Z. I. Almarzooq, A. Alonso, A. Z. Beaton, M. S. Bittencourt, A. K. Boehme, A. E. Buxton, A. P. Carson, Y. Commodore-Mensah *et al.*, "Heart disease and stroke statistics—2022 update: a report from the american heart association," *Circulation*, vol. 145, no. 8, pp. e153–e639, 2022.

[4] R. M. Enoka and J. Duchateau, "Muscle fatigue: what, why and how it influences muscle function," *J Physiol*, vol. 586, no. 1, pp. 11–23, Aug. 2007.

[5] A. J. Buckmire, T. J. Arakeri, J. P. Reinhard, and A. J. Fuglevand, "Mitigation of excessive fatigue associated with functional electrical stimulation," *J Neural Eng*, vol. 15, no. 6, p. 066004, Aug. 2018.

[6] M. O. Ibitoye, N. A. Hamzaid, N. Hasnan, A. K. Abdul Wahab, and G. M. Davis, "Strategies for rapid muscle fatigue reduction during fes exercise in individuals with spinal cord injury: A systematic review," *PLOS ONE*, vol. 11, no. 2, pp. 1–28, 02 2016.

[7] M. Vromans and P. D. Faghri, "Functional electrical stimulation-induced muscular fatigue: Effect of fiber composition and stimulation frequency on rate of fatigue development," *Journal of Electromyography and Kinesiology*, vol. 38, pp. 67–72, 2018, neuromechanics of fine hand-motor tasks.

[8] N. C. Chesler and W. K. Durfee, "Surface EMG as a fatigue indicator during FES-induced isometric muscle contractions," *J Electromyogr Kinesiol*, vol. 7, no. 1, pp. 27–37, Mar. 1997.

[9] R. Pilkar, K. Momeni, A. Ramanujam, M. Ravi, E. Garbarini, and G. F. Forrest, "Use of surface emg in clinical rehabilitation of individuals with sci: Barriers and future considerations," *Frontiers in Neurology*, vol. 11, 2020.

[10] E. Krueger, E. M. Scheeren, G. N. Nogueira-Neto, V. L. d. S. N. Button, and P. Nohama, "Advances and perspectives of mechanomyography," *Revista Brasileira de Engenharia Biomédica*, vol. 30, no. 4, p. 384–401, Oct 2014.

[11] M. A. Islam, K. Sundaraj, R. B. Ahmad, N. U. Ahamed, and M. A. Ali, "Mechanomyography sensor development, related signal processing, and applications: A systematic review," *IEEE Sensors Journal*, vol. 13, no. 7, pp. 2499–2516, July 2013.

[12] M. A. Islam, K. Sundaraj, R. B. Ahmad, and N. U. Ahamed, "Mechanomyogram for muscle function assessment: A review," *PLOS ONE*, vol. 8, no. 3, pp. 1–12, 03 2013.

[13] R. B. Woodward, S. J. Shefelbine, and R. Vaidyanathan, "Pervasive monitoring of motion and muscle activation: Inertial and mechanomyography fusion," *IEEE/ASME Transactions on Mechatronics*, vol. 22, no. 5, pp. 2022–2033, 2017.

[14] K. T. Ebersole, T. J. Housh, G. O. Johnson, T. K. Evetovich, D. B. Smith, and S. R. Perry, "MMG and EMG responses of the superficial quadriceps femoris muscles," *J Electromyogr Kinesiol*, vol. 9, no. 3, pp. 219–227, Jun. 1999.

[15] A. K. Blangsted, G. Sjøgaard, P. Madeleine, H. B. Olsen, and K. Søgaard, "Voluntary low-force contraction elicits prolonged low-frequency fatigue and changes in surface electromyography and mechanomyography," *J Electromyogr Kinesiol*, vol. 15, no. 2, pp. 138–148, Dec. 2004.

[16] S. Solnik, P. Rider, K. Steinweg, P. DeVita, and T. Hortobágyi, "Teager-Kaiser energy operator signal conditioning improves EMG onset detection," *Eur J Appl Physiol*, vol. 110, no. 3, pp. 489–498, Jun. 2010.

[17] Z. Liu, W. Huo, Z. Yu, P. Bentley, A. M. J. Bull, and R. Vaidyanathan, "Continuous estimation of fes-induced neuromuscular fatigue using mechanomyography signals," *IEEE Journal of Biomedical and Health Informatics*, pp. 1–14, 2025.

[18] A. Cudicio, E. Martinez-Valdes, M. Cogliati, C. Orizio, and F. Negro, "The force-generation capacity of the tibialis anterior muscle at different muscle-tendon lengths depends on its motor unit contractile properties," *European Journal of Applied Physiology*, vol. 122, 02 2022.

[19] J. Malešević, L. Konstantinović, G. Bijelić, and N. Malešević, "Smart protocols for physical therapy of foot drop based on functional electrical stimulation: A case study," *Healthcare (Basel)*, vol. 9, no. 5, Apr. 2021.

[20] N. Hayami, H. E. Williams, K. Shibagaki, A. H. Vette, Y. Suzuki, K. Nakazawa, T. Nomura, and M. Milosevic, "Development and validation of a Closed-Loop functional electrical Stimulation-Based controller for gait rehabilitation using a finite state machine model," *IEEE Trans Neural Syst Rehabil Eng*, vol. 30, pp. 1642–1651, Jun. 2022.

[21] Z. Li, D. Guiraud, D. Andreu, A. Gelis, C. Fattal, and M. Hayashibe, "Real-time closed-loop functional electrical stimulation control of muscle activation with evoked electromyography feedback for spinal cord injured patients," *International Journal of Neural Systems*, vol. 28, no. 06, p. 1750063, 2018, pMID: 29378445.

[22] J. M. Wilson, J. P. Loenneke, E. Jo, G. J. Wilson, M. C. Zourdos, and J.-S. Kim, "The effects of endurance, strength, and power training on muscle fiber type shifting," *The Journal of Strength & Conditioning Research*, vol. 26, no. 6, 2012.

[23] W. Scott, J. Stevens, and S. A. Binder–Macleod, "Human skeletal muscle fiber type classifications," *Physical Therapy*, vol. 81, no. 11, pp. 1810–1816, 11 2001.

[24] S. Ferrante, N. Chia Bejarano, E. Ambrosini, A. Nardone, A. M. Turcato, M. Monticone, G. Ferrigno, and A. Pedrocchi, "A personalized Multi-Channel FES controller based on muscle synergies to support gait rehabilitation after stroke," *Front Neurosci*, vol. 10, p. 425, Sep. 2016.

[25] S. Prenton, K. L. Hollands, L. P. Kenney, and P. Onmanee, "Functional electrical stimulation and ankle foot orthoses provide equivalent therapeutic effects on foot drop: A meta-analysis providing direction for future research," *Journal of rehabilitation medicine*, 2017.

[26] D. Smajla, N. Šarabon, A. García Ramos, D. Janicijevic, and Z. Kozinc, "Influence of isometric and dynamic fatiguing protocols on dynamic strength index," *Applied Sciences*, vol. 14, no. 7, 2024.

[27] C. Lynch and M. Popovic, "Closed-loop control for fes: Past work and future directions," in *10th Annual Conference of the International FES Society*. Citeseer, 2005, pp. 2–4.

[28] X. Guo, K. Y. Lau, M. Bai, R. Liu, B. He, J. J. Xie, J. Lin, V. K. Yuen, P. P. Chan, S. L. Law, J. Wang, S. M. Li, C.-H. Chou, C.-y. Chen, G. L. Cheing, P. W. Kwong, N. Lan, R. T. Cheung, R. H. Chan, and V. C. Cheung, "Personalized synergy-based functional electrical stimulation improves lower limb motor functions of chronic stroke survivors by restoring gait control modules," *medRxiv*, 2025.

[29] R. Tamirisa, J. Won, C. Lu, R. Arel, and A. Zhou, "Fedselect: Customized selection of parameters for fine-tuning during personalized federated learning," *arXiv preprint arXiv:2306.13264*, 2023.